JOURNAL OF AIRCRAFT
Vol. 47, No. 2, March–April 2010

Flight Determination of Partial-Span-Flap Parasite Drag with Flap Deflection

David F. Rogers*
U.S. Naval Academy, Annapolis, Maryland 21402

DOI: 10.2514/1.45654

Level-flight performance tests were conducted on a typical light general aviation single-engine retractable aircraft with partially and fully extended partial-span single-slotted flaps in both gear-up and gear-extended configurations. A parabolic variation in the aircraft equivalent parasite drag area with flap deflection was observed for both configurations. A linear relation was discovered between the aircraft equivalent parasite drag area and the *square* of the flap deflection angle for both configurations. This result suggests that level-flight performance tests in the stowed and fully extended flap configurations will yield adequate data for estimating performance for intermediate flap deflections. A similar linear relation was confirmed for an NACA 23012 airfoil equipped with a single-slotted flat using classical NACA wind-tunnel data. The flight tests showed that the aircraft equivalent parasite drag area increased by a factor of 1.16 at 10°, by 1.81 at 20°, and by 3.14 at a full flap deflection of 32° in the gear-up configuration. With the gear extended, the equivalent parasite drag area increased by a factor of 1.14 at 10°, by 1.29 at 20°, and by 1.67 at the 32° full flap deflection. The results are expected to be typical for similar aircraft.

Nomenclature

B	=	slope of the $\mathrm{THP_{req}}V$ vs V^4 line
b	=	wing span
C_{d_o}	=	two-dimensional section drag coefficient
C_ℓ	=	two-dimensional section lift coefficient
c	=	airfoil or wing chord
e	=	Oswald efficiency factor
f	=	aircraft equivalent parasite drag area
R^2	=	square of the correlation coefficient
S	=	wing reference area
$\mathrm{THP_{req}}$	=	thrust horsepower required
$\mathrm{THP_{req_{std}}}$	=	thrust horsepower required at standard weight and altitude
V	=	true airspeed
V_{std}	=	true airspeed at standard weight and altitude
W	=	weight of the aircraft
δ_f	=	flap deflection angle
ρ	=	density
ρ_{SL}	=	density at sea level
σ	=	ratio of the density at altitude to that at sea level, ρ/ρ_{SL}

Introduction

VARIOUS lift-enhancing devices are used to increase the operational speed range of aircraft, particularly at the low end near stall. Lower stall speeds decrease the landing distance. Fundamentally, there are only three techniques available for increasing the lift on an airfoil: camberline change, boundary-layer control, and area increase. Deflecting a trailing-edge flap, drooping the leading edge of an airfoil, or adding an external downward-deflected leading-edge slat are examples of devices that change the camber of the airfoil. Fixed leading-edge slots, extensible leading-edge slats, and single- or multiple-slotted trailing-edge flaps, as well as direct boundary-layer blowing or suction, are examples of lift-enhancing devices that use boundary-layer control. Fowler and multiple-slotted trailing-edge flaps and extensible leading-edge slats are devices that depend on increasing area to enhance lift. Obviously, individual devices may use multiple methods for lift enhancement. Modern wing design typically incorporates both leading-edge and trailing-edge devices at the expense of additional mechanical complexity.

Typically, light general aviation aircraft of less than 6000 lb depend on trailing-edge flaps for lift enhancement. Full deflection of trailing-edge flaps is used to increase the approach and landing descent angles. Fully or partially deflected flaps may be used as speed brakes. Because small flap deflections result in proportionally greater increases in lift than in drag, partial flap extension may be used to decrease the takeoff distance. Partial flap extension may also be used to decrease the maneuvering turn radius. For multi-engine aircraft, partial flap extension lift and drag characteristics are important for single-engine climb performance. Typically, only partial-span flaps are used because the trailing edge is also used for lateral control devices.

A literature review revealed several early NACA technical reports, wartime reports, and technical notes reporting wind-tunnel experiments on NACA 230 mean line airfoils with slotted flaps, as well as a number of experiments on finite wings with full- or partial-span slotted flaps. The works of Wenzinger and Harris [1] and House [2] are representative of these efforts and particularly germane to the present study.

The experiments by Wenzinger and Harris [1] compare and evaluate the characteristics of an NACA 23012 airfoil with $0.2c$ split and plain flaps, along with a $0.2667c$ external airfoil, Fowler, and various single-slotted flaps. They found that an optimum single-slotted flap provided a superior maximum lift coefficient compared to split, plain, and external airfoil flaps. However, the slot had to be carefully shaped and positioned to achieve optimal results. A Fowler flap provided a slightly higher maximum lift coefficient than the optimal single-slotted flap, but at the expense of additional complexity.

House [2] investigated the effects of center- and tip-located partial-span flaps on finite wings of aspect ratio six. He concluded that center span flaps had higher values of maximum lift coefficient and that the values of maximum lift coefficient did not significantly change with an increase in flap span beyond $0.40b$.

Aircraft

The flight tests were conducted in an E33A Beech Bonanza. A three-view drawing is shown in Fig. 1. The aircraft had

Received 25 May 2009; accepted for publication 6 August 2009.

*Professor Emeritus, Aerospace Engineering Department, 590 Holloway Road, Annapolis, Maryland 21402; dfr@nar-associates.com. Associate Fellow AIAA.

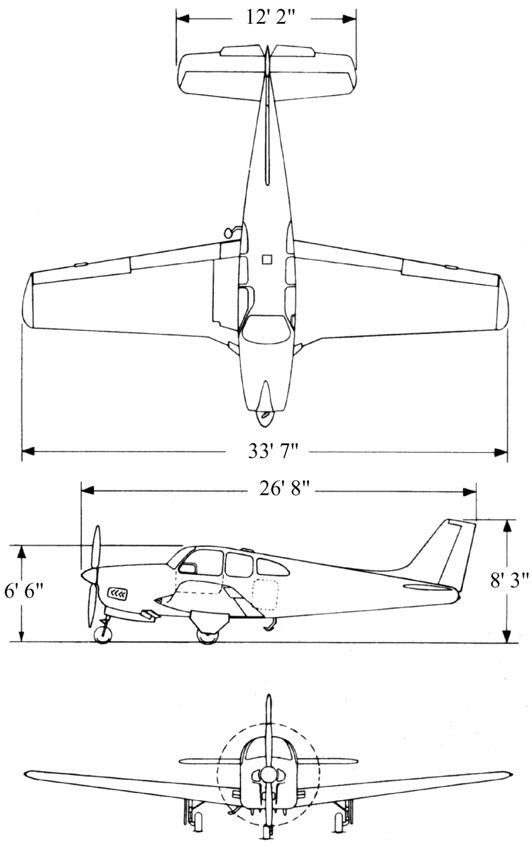

Fig. 1 E33A Beech Bonanza three-view drawing.

approximately 600 h on a recently installed Teledyne Continental Motors IO-520BB 285 BHP factory-remanufactured six-cylinder fuel-injected engine. The aircraft has a fuel computer capable of measuring and displaying fuel flow and fuel remaining. The aircraft empty weight is 2142 lb, including the weight of 6 gal of unusable fuel and 10 qt of oil. The aircraft is equipped with a recently overhauled McCauley three-blade propeller (3A32C76 hub with 82NB-2 blades) with a nominal diameter of 80 in. The aircraft is fitted with a Century II autopilot and panel-mounted instrument-flight-rules-certified Global Positioning System (GPS) avionics along with an S-TEC PSS60 altitude hold. This equipment was used for the flight tests. This particular aircraft has the speed sweep windshield to reduce drag. Improved engine baffling for better engine cooling and reduced cooling drag has also been fitted. In addition, the Beechcraft bird-wing antennas have been removed to further reduce drag. The aircraft is shown in Rogers [3].

Wing

The aircraft wing span is 33.6 ft including wing tips (see Fig. 2). Höerner wing tips are fitted. The straight tapered wing has a taper ratio of 0.5. The quarter-chord of the wing is unswept. The theoretical airfoil at the centerline of the aircraft is an NACA 23016.5 with a chord of 84 in. The airfoil at the wing tip is an NACA 23012. The modified leading-edge extension (LEX) at the aircraft centerline extends forward of the quarter-chord by 37.6 in. to yield a theoretical centerline chord of 100.6 in. The leading edge of the LEX extends in a straight line from the leading edge of the theoretical centerline airfoil to intersect the leading edge of the straight tapered wing at station 47 to form a crank in the wing. There is a triangular spin strip at the crank of the wing. There is also a small 7.875-in.-long triangular spin strip on the wing centered at wing station 70.4375. The wing has 3° of washout varying linearly from the theoretical root section to the tip. The wing dihedral is 6°. The reference wing area is 181 ft^2, which yields a reference aspect ratio of 6.2.

Flap

The single-slotted flap extends from the fuselage sidewall outboard along the wing to station 109.3 (inches from the aircraft centerline), as shown in Fig. 2. The flap chord at the inboard end is 20.0 in. and at the outboard end is 15.1 in. The individual flap span measured at the flap quarter-chord is 87.2 in., which equates to $0.43b$. The planform area of an individual flap is 10.6 ft^2. The slot is well formed. Flap deflection was measured at station 29 approximately 5 in. outboard of the fuselage at the undeflected flap trailing edge. Both a manual jig and protractor and a digital inclinometer were used to measure the deflection. Maximum deflection was measured as 32° at this location.

Initially, the flap moves aft and down along an internal track (see Fig. 3), The maximum aft movement of 2.315 in. occurs at 20° of flap deflection, which effectively adds 33.6 ft^2 to the wing area. At full flap deflection the trailing edge moves downward and forward from the 20° position to 2 in. aft of the stowed position.

Flight Tests

The flight tests were conducted at a pressure altitude of 6000 ft. A box pattern was flown in order to acquire data for the horseshoe

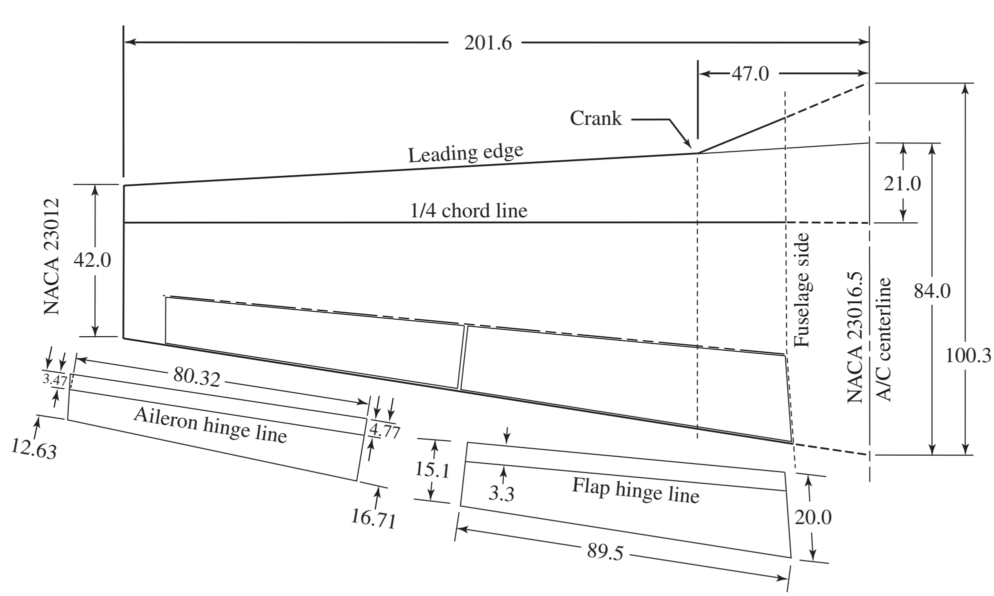

Fig. 2 Wing schematic.

Fig. 3 Wing flap slot and track.

heading technique used to determine the true airspeed from the GPS ground speed [4]. Constant brake horsepower settings from 38 to 75% were used to set the airspeed for each data run and to remain below the maximum flap extension speed. The aircraft tachometer was calibrated against a stroboscopic tachometer and thereafter used to measure propeller rpm. The aircraft instrument was used to measure engine manifold pressure in order to determine power available. Mixture was set to correspond to best power [5] (i.e., approximately 100° rich of peak exhaust gas temperature). During the flight tests, aircraft weight varied from 3179 to 2669 lb for the various flights. Outside air temperature (OAT) varied from 32 to 52°F for the various data runs. Typically, the OAT remained nearly constant for each data run. Manifold pressure varied from approximately 18.2 to 23.2 in. Hg in 0.5 to 1 in. Hg increments. Propeller speed varied from approximately 1850 to 2500 rpm in approximately 100 rpm increments. The gear- and flap-retracted-configuration flight tests were conducted with cowl flaps and all cabin vents closed. The gear-down tests were conducted with cowl flaps open and all cabin vents closed. Typically, five or six data points were obtained for each flap setting during a single flight.

Data Acquisition and Reduction

The true airspeed was determined using the horseshoe heading technique as detailed by Rogers [4] and the references therein. This technique has been shown to be as accurate, within less than ±1 kt, as a traditional trailing cone or Kiel tube [6]. Basically, the flight test consists of flying three legs with headings 90° apart while recording the GPS ground speed. Using these GPS ground speeds and headings and solving three algebraic equations in three unknowns yields the true airspeed, wind direction, and wind speed.

Aircraft weight was determined by subtracting the fuel used as determined by the onboard fuel computer from the aircraft gross weight before engine start. Atmospheric density was determined from measured outside air temperature and the pressure altitude. Engine brake horsepower was determined from the manufacturer's engine charts [5] for best power mixture using measured manifold pressure and engine rpm. The propeller efficiency was calculated from polynomial curves determined from the manufacturer's propeller map [7]. The results were reduced to a standard gross weight of 3300 lb at sea level using true airspeed and the technique described in Appendix A of Rogers [3]. The results of these flight tests are shown in Figs. 4–6.

Results

Recalling the classical thrust-power-required equation for an aircraft with a parabolic drag polar equipped with a reciprocating engine driving a propeller,

$$\mathrm{THP}_{\mathrm{req}} = \underbrace{\frac{\sigma\rho_{\mathrm{SL}}}{2} f V^3}_{\text{parasite}} + \underbrace{\frac{2}{\sigma\rho_{\mathrm{SL}}}\frac{1}{\pi e}\left(\frac{W}{b}\right)^2 \frac{1}{V}}_{\text{effective induced}} \tag{1}$$

Multiplying by the true airspeed yields

$$\mathrm{THP}_{\mathrm{req}} V = \frac{\sigma\rho_{\mathrm{SL}}}{2} f V^4 + \frac{2}{\sigma\rho_{\mathrm{SL}}}\frac{1}{\pi e}\left(\frac{W}{b}\right)^2 \tag{2}$$

which is a linear relation in V^4. Hence, the aircraft equivalent parasite drag area is obtained from the slope of the straight line. As used here, the aircraft equivalent parasite drag area is simply the classical parabolic drag polar constant term (i.e., the zero-lift drag coefficient) multiplied by the aircraft reference wing area.

Figure 4 shows the data plotted as $\mathrm{THP}_{\mathrm{req}_{\mathrm{std}}} V$ against V^4 as suggested by Eq. (2). A linear least-squares fit is also shown for each flap deflection. Clearly, the expected linear relation results. The increased slope for the aircraft with increasing flap deflection indicates increased equivalent parasite drag as expected. Table 1 shows the values for the slope, B, the R^2 value, and the value f obtained using Eq. (2). The results in Table 1 show that, as expected, increasing flap deflection increases the equivalent parasite drag area.

The equivalent parasite drag area plotted against flap deflection is shown in Fig. 5. The parabolic least-squares fit to the data, also shown in Fig. 5, clearly indicates that the equivalent parasite drag area varies parabolically with flap deflection.

The parabolic variation of the equivalent parasite drag area with flap deflection suggests a linear variation with the square of the flap deflection. Figure 6 shows the equivalent parasite drag area for the flight-test data plotted against the square of the flap deflection in radians, along with a linear least-squares fit to the data of Table 1.

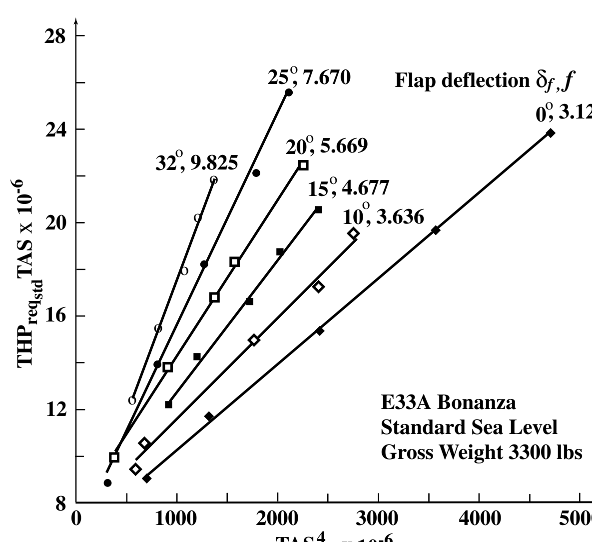

Fig. 4 Equivalent parasite drag area for various flap deflections.

Table 1 Results for f gear up

δ_f°	$B \times 10^3$	R^2	f, ft^2	Δf, ft^2
0	3.714	0.995	3.125	0.000
10	4.321	0.991	3.636	0.511
15	5.556	0.992	4.677	1.552
20	6.737	0.998	5.669	2.544
25	9.116	0.997	7.670	4.545
32	11.676	0.996	9.825	6.700

Table 2 Results for f with gear down and cowl flaps open

δ_f°	$B \times 10^3$	R^2	f, ft^2	Δf, ft^2
0	8.808	0.9897	7.593	4.286
10	10.276	0.9711	8.646	5.521
20	11.681	0.9995	9.829	6.522
32	15.114	0.9932	12.717	9.592

McCormick [8] (Table 4.2) gives the skin-friction coefficient for a model V-35 V-tail Bonanza as 0.0049. Eckalbar [9] gives the wetted surface area as estimated by Stinton [10] as 620 ft^2 for the V-35 and estimates that the wetted surface area of the conventional-tailed model E33A as 620 ft^2. Using McCormick's [8] value for the skin-friction coefficient and Eckalbar's [9] estimate for the wetted surface area yields an equivalent parasite drag area of 3.14 ft^2, which agrees quite well with the current flight-test result for $\delta_f = 0$ of 3.125 ft^2.

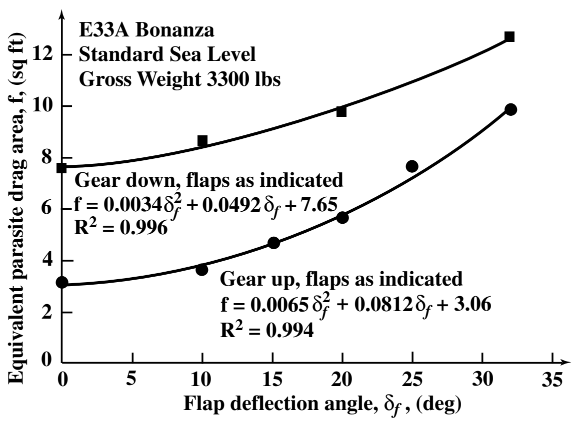

Fig. 5 Equivalent parasite drag area as a function of flap deflection angle δ_f.

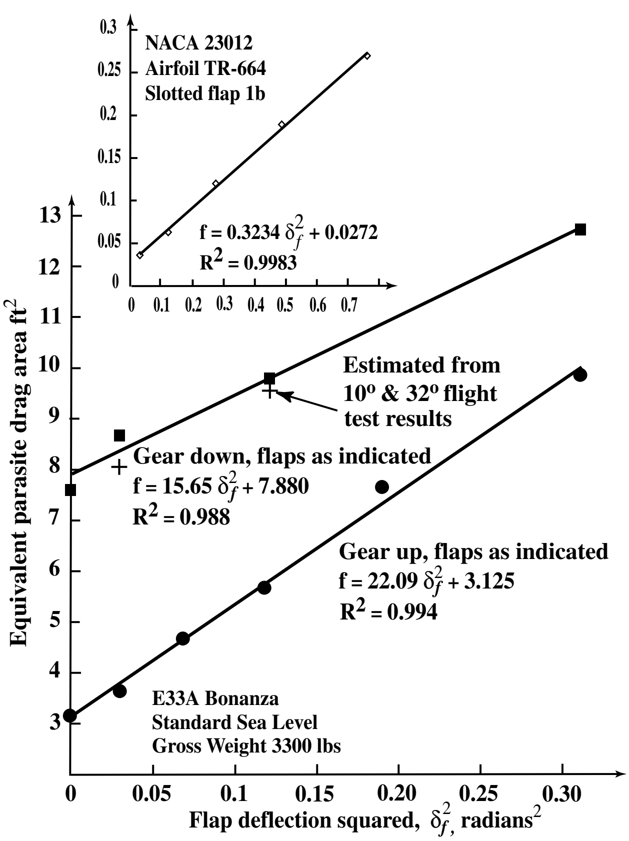

Fig. 6 Equivalent parasite drag area as a function of the square of the flap deflection angle δ_f^2.

A literature search revealed no similar flight-test data for partial-span partially deflected flaps. However, Wenzinger and Harris [1] present wind-tunnel airfoil data for an NACA 23012 airfoil equipped with a 0.2566-chord slotted flap, although they do not plot the data versus δ_f^2. Extracting the data from Wenzinger and Harris [1] (Fig. 15) for C_{d_0} at $C_l = 0$ for flap deflections from 0 to 40° and performing a linear least-squares fit again yields a linear relation in the square of the flap deflection, as shown in the inset in Fig. 6. Data from Wenzinger and Harris for split, plain, and Fowler flaps also yield a linear relation in the square of the flap deflection for similar flap deflection angles, although the slopes are, not surprisingly, different. This result suggests that two or three level-flight performance tests with partially extended flaps will yield adequate data for estimating performance for modest flap deflections.

To test the preceding suggestion, four additional flight tests were conducted with gear down and cowl flaps open with various flap deflections. The results are shown in Table 2 and in Fig. 6. The first flight test was conducted with gear down and a flap deflection of zero. The second flight test was conducted with gear down and a flap deflection of 32°. Using a linear fit based on the equivalent parasite drag area versus flap deflection squared derived from these two initial flight-test results, the equivalent parasite drag area for gear-down and flap deflections of 10 and 20° was estimated. The estimated values are shown by the $+s$ in Fig. 6. Flight tests were then conducted with flap deflections of 10 and 20°. The flight-test results are shown by the squares in Fig. 6. The flight-test results are in good agreement with the estimates.

An additional flight test was conducted to determine the effect of open cowl flaps. The results show that open cowl flaps increase the equivalent parasite drag area by 0.18 ft^2.

Conclusions

Level-flight performance tests were conducted on a typical light general aviation single-engine retractable aircraft to determine the equivalent parasite drag area of partially deflected partial-span flaps. The equivalent parasite drag area in the gear-up configuration increased by a factor of 1.16 for a 10° flap deflection angle and by a factor of 1.81 for a 20° flap deflection angle compared to zero flap deflection. At a maximum deflection of 32° the aircraft equivalent parasite drag area increased by a factor of 3.14 compared to the aircraft value when the flaps were undeflected. With the gear extended, the equivalent parasite drag area increased by a factor of 1.14 at 10°, by a factor of 1.29 at 20°, and by a factor of 1.67 at the 32° full flap deflection compared to the zero-flap gear-extended results. Both a parabolic variation of the equivalent parasite drag area with flap deflection angle and a linear relation with the flap deflection angle squared were found for both configurations. Additional flight tests in the gear-down configuration confirmed the linear variation with flap deflection angle squared. Classical NACA wind-tunnel data for an NACA 23012 airfoil equipped with a similar single-slotted flap also resulted in both a parabolic variation of the equivalent parasite drag area with flap deflection angle and a linear relation with flap deflection angle squared. The results are expected to be similar for similar aircraft.

References

[1] Wenzinger, C. J., and Harris, T. A., "Wind-Tunnel Investigation of an NACA 23012 Airfoil with Various Arrangements of Slotted Flaps," NACA Rept. 664, 1939.

[2] House, R. O., "The Effects of Partial-Span Slotted Flaps on the Aerodynamic Characteristics of Rectangular and Tapered NACA 23012 Wing," NACA TN-719, 1939.

[3] Rogers, D. F., "Comparative Flight Tests with and Without Tip Tanks," *Journal of Aircraft*, Vol. 44, No. 5, Sept.–Oct. 2007, pp. 1740–1744. doi:10.2514/1.30698

[4] Rogers, D. F., "An Engineering Flight Test Course Emphasizing Flight Mechanics Concepts," *Journal of Aircraft*, Vol. 39, No. 1, Jan.–Feb. 2002, pp. 79–83. doi:10.2514/2.2898

[5] *IO-520 Series, Operator's Manual*, Form X30041, Teledyne Continental Motors, Aircraft Products Div., Mobile, AL, Sept. 1980.

[6] Lewis, G., "A Flight Test Technique Using GPS for Position Error Correction Testing," *Cockpit*, Jan.–March 1997, pp. 20–24.

[7] *McCauley D3A32C88/82NC-2 Propeller Chart*, Cessna Aircraft Co., McCauley Accessory Div., Vandalia, OH.

[8] McCormick, B., *Aerodynamics, Aeronautics and Flight Mechanics*, Wiley, New York, 1979.

[9] Eckalbar, J., *Flying the Beech Bonanza*, McCormick-Armstrong, Wichita, KS, 1986.

[10] Stinton, D., *The Design of the Airplane*, 2nd ed., AIAA, Reston, VA, 2001.